Extrinsic screening of ferroelectric domains in $Pb(Zr_{0.48}Ti_{0.52})O_3$

I. Krug, N. Barrett, A. Petraru, A. Locatelli, T. O. Mentes, M. A. Niño, K. Rahmanizadeh, G. Bihlmayer, and C. M. Schneider

Citation: Appl. Phys. Lett. **97**, 222903 (2010);
View online: https://doi.org/10.1063/1.3523359
View Table of Contents: http://aip.scitation.org/toc/apl/97/22
Published by the American Institute of Physics

Extrinsic screening of ferroelectric domains in $Pb(Zr_{0.48}Ti_{0.52})O_3$

I. Krug,[1] N. Barrett,[2,a)] A. Petraru,[3] A. Locatelli,[4] T. O. Mentes,[4] M. A. Niño,[4] K. Rahmanizadeh,[5] G. Bihlmayer,[5] and C. M. Schneider[1]
[1]*IFF-9 and JARA-FIT, Research Center Jülich GmbH, D-52425 Jülich, Germany*
[2]*CEA, IRAMIS, SPCSI, LENSIS, F-91191 Gif-sur-Yvette, France*
[3]*Inst. f. Elektrotechnik u. Informationstechnik/Nanoelektronik, University Kiel, D-24143 Kiel, Germany*
[4]*Sincrotrone Trieste S.C.p.A., S.S. 14 Km 163.5, I-34149 Basovizza, Italy*
[5]*IFF-1 and IAS-1, Research Center Jülich GmbH, D-52425 Jülich, Germany*

(Received 15 October 2010; accepted 11 November 2010; published online 2 December 2010)

The variation in the surface potential as a function of the ferroelectric polarization of micron scale domains in a thin epitaxial film of $Pb(Zr_{0.48}Ti_{0.52})O_3$ is measured using mirror electron microscopy. Domains were written using piezoforce microscopy. The surface potential for each polarization was deduced from the mirror to low energy electron microscopy transition in the local reflectivity curve. The effect of extrinsic screening of the fixed polarization charge at the ferroelectric surface is demonstrated. The results are compared with density functional theory calculations. © *2010 American Institute of Physics*. [doi:10.1063/1.3523359]

At a boundary of a ferroelectric (FE) material, the atomic polarization induces a surface charge σ given by $\sigma = \vec{P} \cdot \vec{n}$, where $\vec{P}$ is the polarization vector and $\vec{n}$ is the unit vector normal to the surface. This surface charge creates a depolarizing electric field pointing opposite to the field generated by the internal FE polarization. It may be screened by charge carriers or defects in the bulk or by external charges from adsorbate species. In nanoscale films, the charge state of a FE surface can dominate the film properties even in deeper layers and impose ultimate limits on polarization and thickness.[1]

Screening of the fixed polarization charge at the surface will result in a change in the surface potential modulating the surface properties. Li *et al.* showed polarization dependency for reactive sticking coefficients on BTO and $Pb(Zr_{0.48}Ti_{0.52})O_3$ (PZT).[2] The authors also demonstrated that the effect of molecular adsorption was to attenuate but not fully screen the potential differences between the differently poled regions. Fong *et al.* showed that OH adsorption stabilizes monodomain state in epitaxial $PbTiO_3$ films.[3] Near-field techniques such as piezoforce or scanning surface potential microscopy can probe such modifications.[4]

Detrimental tip-surface interactions inherent to scanning probe microscopy may be avoided by using an alternative approach mirror electron microscopy (MEM),[5] which allows full-field imaging of the surface topography and potential[6] and has recently been applied to FE domains.[7] By using reflected electrons, MEM minimizes possible surface charging and low energy electron induced oxygen desorption.[8] Therefore, we have chosen to probe the transition from the mirror reflection of the electrons to the back scattering regime, commonly referred to as the MEM-LEEM (low energy electron microscopy) transition. MEM is highly sensitive to the local variations of the surface potential, as small differences in the latter determine large differences in the electron reflectivity.[9] Thus, the energy of the MEM-LEEM transition provides an accurate nondestructive map of the charge state or screening of the surface of FE domains.

A (001)-oriented PZT layer was grown by high pressure sputtering on conducting $SrRuO_3$ (SRO) back electrode which itself is deposited on $SrTiO_3(001)$ single crystal substrate. The PZT stoichiometry was chosen near the morphotropic phase boundary to assure a maximum piezoelectric response.[10] The layer thickness of 30 nm is below the threshold for strain relaxation, ensuring a low defect density and a high polarization normal to the sample plane. The PZT layer was covered with a platinum mask with open fields to facilitate the location of the FE domains. In addition, the mask provides energy calibration of the photoemission spectra with respect to the Pt 4f peaks and the Fermi level.

The sample was polarity-patterned in the open fields of the Pt mask by piezoforce microscopy (PFM), first by a writing step with a conductive tip held at a dc bias voltage, followed by a reading step applying a smaller voltage for the piezoresponse pickup. Both steps have been performed without any alteration of the surface checked by PFM topography images (not shown). The outer square of 10×10 μm was written by a positive bias of +5 V creating a negative image charge below the surface and thus a P^- state (inward directed polarization). The polarity of an inner 5×5 μm square was reversed by a -5 V bias (P^+). The exterior, i.e., unwritten sample area, exhibits a net positive polarity probably due to a FE imprint in the film after growth and cooling to room temperature.

The experiments hereafter reported were carried out using the SPELEEM microscope[11] installed on the Nanospectroscopy beam line at the ELETTRA synchrotron laboratory in Trieste.[12] The SPELEEM is a multimethod spectromicroscopy that combines x-ray photoelectron emission microscopy (XPEEM) with LEEM and MEM.[13]

The poled PZT pattern was studied before and after cleaning of the surface contamination. Cleaning was achieved by *in situ* annealing in oxygen. The most efficient conditions were found to be O_2 partial pressure of 4.8×10^{-5} mbar at 400 °C for several hours. Lower oxygen partial pressures had a little effect on the surface contamination. The surface contamination was monitored in the PEEM by the O and C 1s core levels and the valence band with photon energies of 700 and 312 eV, respectively. The spectra

a)Electronic mail: nick.barrett@cea.fr.

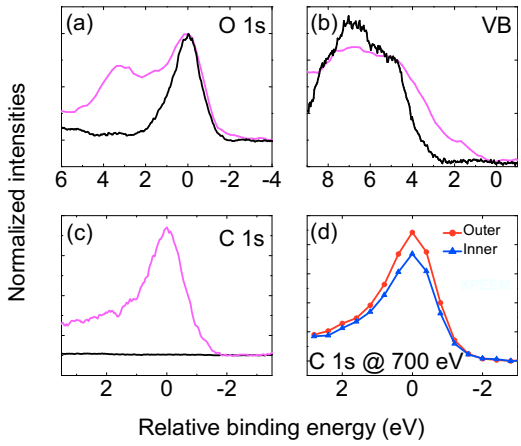

FIG. 1. (Color online) [(a)–(c)] O 1s, valence band, and C 1s photoemission spectra averaged over the field of view before (light gray) and after (black) annealing in oxygen. (d) XPEEM C 1s map of as-received PZT across a field of view of 15 μm for P^+ (triangles) and P^- (circles) domains.

averaged over the field of view containing the P^+/P^- written domain structure are shown in Figs. 1(a)–1(c).

Before annealing, the O 1s spectrum has a strong contribution at a binding energy of ~2 eV higher than the component due to oxygen in the PZT lattice. This is most probably due to chemisorption of CO_2 at an on-top surface oxygen site.[2,14] There is a correspondingly strong C 1s signal. The valence band is dominated by the O 2p levels but also shows a significant density of states up to the Fermi level, again a characteristic of the presence of surface carbon. There is evidence for a higher carbon signal on the P^- polarized domain than on the P^+ and the unwritten areas [Fig. 1(d)]. After annealing, the high binding energy component in the O 1s spectrum attributed to a carbonate-like state disappears as does the C 1s signal, indicating that the oxygen annealing has removed the carbon-based contamination. The valence band after cleaning is close to that expected for clean PZT. A gap clearly shows up between 0 and 2.6 eV below the Fermi level, confirming that the contamination of the PZT surface, responsible for gap states, has been eliminated.

Figure 2(a) compiles images from the clean sample obtained over the MEM-LEEM transition. There is a clear contrast inversion with kinetic energy, indicating a polarization dependent surface potential.

Figures 2(b) and 2(c) show the reflectivity curves extracted from the regions of interest marked in the inset of Fig. 2(c). The polarity of the different domains clearly influences the energy of the MEM-LEEM transition. For each polarity, two regions of interest were defined in order to avoid spurious intensity effects and the average curve of the two regions is plotted. The squares are aligned perpendicular to the analyzer dispersive direction to avoid any energy shift or broadening. All images have been normalized with respect to the flat field to eliminate contributions due to inhomogeneities in the detection system. The MEM-LEEM transitions as obtained from the midpoint of the decrease in the reflectivity curves are reported in Table I.

For the as-received surface, the spread in the energy of the MEM-LEEM transition as a function of the FE domain polarization is less than 60 meV between the P^+ and P^- domains. This indicates that the fixed polarization charge has been screened. The core level and valence spectra suggest that extrinsic screening due to surface contamination domi-

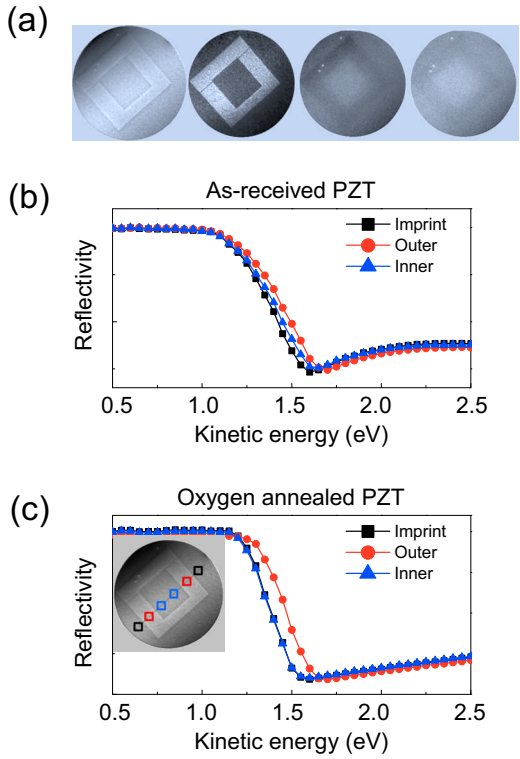

FIG. 2. (Color online) (a) Images of the PFM-written FE domains for kinetic energy across the MEM-LEEM transition (from left to right: 0.8, 1.45, 1.85, and 2.45 eV). The inner square is P^+, the outer is P^-, and the unwritten PZT film has an imprint FE polarization. Local electron reflectivity curves extracted from the regions of interest in the inset (b) before and (c) after *in situ* surface annealing in oxygen.

nates. After cleaning, the dispersion in surface potential values increases to 90 meV. Furthermore, there is a clear distinction in the energy of the MEM-LEEM transition between P^+ and P^- written domains. The transition for the unwritten area in the field of view is extremely close to that of the P^+ domain confirming the PFM observation that the thin PZT film has a positive FE imprint, already observed for epitaxial PZT on SRO.[15] The fact that the effect of cleaning is stronger on the P^- domain is consistent with our observation of a heterogeneous carbon distribution.

We compare our results to density functional theory (DFT) calculations in the generalized gradient approximation.[16] The results were obtained using the full potential linearized augmented plane wave method as implemented in the FLEUR code.[17] X-ray photoelectron spectroscopy (not shown) confirms that the PZT is mainly PbO terminated. The surface was simulated by a PbO terminated nine-layer $PbTiO_3$ film embedded in vacuum with the polarization perpendicular to the surface stabilized by an external

TABLE I. Energy of MEM-LEEM transition as measured from the reflectivity curves of Fig. 2.

	MEM-LEEM transition (eV)	
	Contaminated	Clean
P^+	1.38	1.37
P^-	1.43	1.46
Unwritten	1.37	1.37

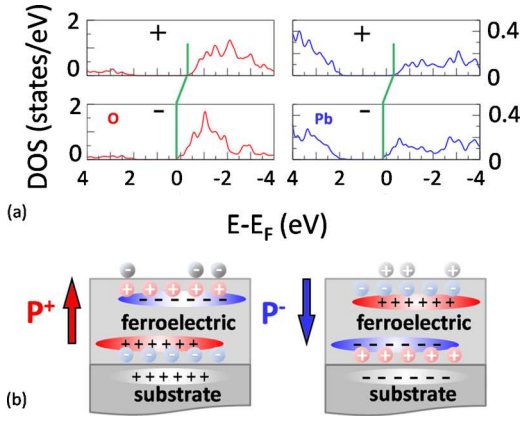

FIG. 3. (Color online) (a) O 2p and Pb partial density of states calculated for a nine layer slab of polarized PTO with the predicted P^+/P^- offset. (b) Schematic of slabs showing the possible intrinsic (black + or −) and extrinsic (white + or − on gray adsorbates) screening charge of the fixed polarization charge (white + or − in ferroelectric).

electric field. The results for the O and Pb projected density of states for the top and bottom sides of the slab (P^+ and P^- terminations, respectively) are shown in Fig. 3(a). The theory predicts that the conduction band (CB) for the P^+ surface is 0.5 eV higher than that for the P^- surface. At constant electron affinity, this should translate into a similar work function difference, as already observed.[18] An electron approaching the surface from outside the sample will therefore encounter a similar potential barrier but from the vacuum side. The P^+ surface should exert a greater attractive potential than the P^- surface. Thus, the MEM-LEEM transition should occur at a lower start voltage for a P^+ surface than for a P^- surface. We measure a difference of 0.1 eV in the MEM-LEEM transition. Since the theoretical slab is screened only by an external electric field, the calculations rather provide upper limits to the photoionization thresholds. They do not include extrinsic (adsorbate) or intrinsic (charge carriers in the PZT) screening, shown in a schematic band bending model in Fig. 3(b). The former qualitatively explains the narrow spread of the transition energy in Fig. 2(b). The latter may explain the smaller difference between the experimental MEM-LEEM transitions and the CB offset estimated from the DFT calculations. However, we only observed diffuse low energy electron diffraction patterns on the clean surface, thus the small magnitude of the polarization dependent shift in the MEM-LEEM transition compared to theory may also be due to surface disorder.

We have measured the MEM-LEEM transition as a function of the FE polarization of PFM written domains in PZT. A clear difference in surface potential is observed between P^+ and P^- domains. The screening effect of surface contamination is demonstrated. The results are explained within the framework of a qualitative model based on consideration of the image charge potential and are supported by DFT calculations.

[1]J. Junquera and P. Ghosez, Nature (London) **422**, 506 (2003).
[2]D. Li, M. H. Zhao, J. Garra, A. M. Kolpak, A. M. Rappe, D. A. Bonnell, and J. M. Vohs, Nature Mater. **7**, 473 (2008).
[3]D. D. Fong, A. M. Kolpak, J. A. Eastman, S. K. Streiffer, P. H. Fuoss, G. B. Stephenson, C. Thompson, D. M. Kim, K. J. Choi, C. B. Eom, I. Grinberg, and A. M. Rappe, Phys. Rev. Lett. **96**, 127601 (2006).
[4]S. V. Kalinin and D. A. Bonnell, Phys. Rev. B **63**, 125411 (2001).
[5]G. Bartz, G. Weissenberg, and D. Wiskott, Proceedings of the Fourth International Conference on Electron Microscopy, London, 1954, p. 395.
[6]W. Swiech, B. Rausenberger, W. Engel, A. M. Bradshaw, and E. Zeitler, Surf. Sci. **294**, 297 (1993).
[7]S. Cherifi, R. Hertel, S. Fusil, H. Béa, K. Bouzehouane, J. Allibe, M. Bibes, and A. Barthélémy, Phys. Status Solidi (RRL) **4**, 22 (2010).
[8]O. Dulub, M. Batzilln, S. Solovev, E. Loginova, A. Alchagirov, T. E. Madey, and U. Diebold, Science **317**, 1052 (2007).
[9]S. A. Nepijko, N. Sedov, and G. Schönhense, J. Microsc. **203**, 269 (2001).
[10]J. Rodríguez Contreras, H. Kohlstedt, A. Petraru, A. Gerber, B. Hermanns, H. Haselier, N. Nagarajan, J. Schubert, U. Poppe, Ch. Buchal, and R. Waser, J. Cryst. Growth **277**, 210 (2005).
[11]A. Locatelli, L. Aballe, T. O. Mentes, M. Kiskinova, and E. Bauer, Surf. Interface Anal. **38**, 1554 (2006).
[12]For SPLEEM specifications see http://www.elettra.trieste.it/beamlines/nasp/.
[13]T. Schmidt, S. Heun, J. Slezak, J. Diaz, K. C. Prince, G. Lilienkamp, and E. Bauer, Surf. Rev. Lett. **5**, 1287 (1998).
[14]J. D. Baniecki, M. Ishii, K. Kurihara, K. Yamanaka, T. Yano, K. Shinozaki, T. Imada, and Y. Kobayashi, J. Appl. Phys. **106**, 054109 (2009).
[15]P. Maksymovych, S. Jesse, P. Yu, R. Ramesh, A. P. Baddorf, S. V. Kalinin, and I. J. Busch-Vishniac, Science **324**, 1421 (2009).
[16]Z. Wu and R. E. Cohen, Phys. Rev. B **73**, 235116 (2006).
[17]For a description of the code, see http://www.flapw.de.
[18]N. Barrett, J. Rault, I. Krug, B. Vilquin, G. Niu, B. Gautier, D. Albertini, P. Lecoeur, and O. Renault, Surf. Interface Anal. **42**, 1690 (2010).